ARTHRITIS & RHEUMATISM
Vol. 63, No. 9, September 2011, pp 2584–2594
DOI 10.1002/art.30439

Reduction of In Vitro Invasion and In Vivo Cartilage Degradation in a SCID Mouse Model by Loss of Function of the Fibrinolytic System of Rheumatoid Arthritis Synovial Fibroblasts

Simona Serratì,[1] Francesca Margheri,[1] Anastasia Chillà,[1] Elena Neumann,[2] Ulf Müller-Ladner,[2] Maurizio Benucci,[3] Gabriella Fibbi,[1] and Mario Del Rosso[1]

Objective. **Urokinase plasminogen activator (uPA), uPA receptor (uPAR), and PA inhibitor 1 (PAI-1) have pivotal roles in the proliferation and invasion of several cell types, including synovial fibroblasts (SFs). The aim of this study was to investigate the possibility of controlling the invasion of rheumatoid arthritis (RA) SFs in vitro and in vivo by inhibiting uPA and uPAR.**

Methods. **Normal SFs, SFs from patients with RA, and SFs from patients with psoriatic arthritis (PsA) were used. The levels of uPA, uPAR, and PAI-1 were measured by enzyme-linked immunosorbent assay and reverse transcription–polymerase chain reaction analysis of messenger RNA. The activity of uPA was studied by zymography. Proliferation was measured by cell counting, and cell invasion was measured with a Boyden chamber assembled with Matrigel-coated porous filters. Human cartilage and RA SF implantation in the SCID mouse model of RA were used to study cartilage invasion in vivo.**

Results. **RA SFs and PsA SFs overexpressed uPAR and as a result were more active than their normal counterparts in terms of both Matrigel invasion and proliferation. This effect was counteracted by a specific inhibitor of uPA enzymatic activity (WX-340) and by uPAR antisense treatment. The use of both WX-340 and uPAR antisense treatment in vitro showed cooperative effects in RA SFs that were more intense than the effects of either treatment alone. Significant inhibition of cartilage invasion was obtained in vivo with uPAR antisense treatment, while uPA inhibition was inefficient, either alone or in combination with antisense treatment.**

Conclusion. **The decrease in uPAR expression in RA SFs reduced invasion of human cartilage in vitro and in the SCID mouse model.**

Rheumatoid arthritis (RA) is a chronic inflammatory joint disease characterized by hypertrophic synovitis and bone erosion. Resident and inflammatory joint cells produce enzymes that sustain the process of synovial pannus–driven extracellular proteolysis and proliferation (1). Excessive proteolysis also characterizes neoplastic cell invasion (2) and tumor- or inflammation-associated angiogenesis (3). The plasminogen activator (PA) and matrix metalloproteinase (MMP) systems represent the main proteases involved in the invasion and degradation of anatomic barriers.

Urokinase PA (uPA) interacts with its receptor (uPAR) and activates the proenzyme plasminogen to the serine protease plasmin. Plasmin degrades extracellular matrix both directly and indirectly through activation of soluble proMMPs (1). The generation of plasmin from plasminogen is controlled by PA inhibitors (PAIs), and the activity of plasmin is in turn regulated by specific

Supported by Ente Cassa di Risparmio di Firenze and Istituto Toscano Tumori.

[1]Simona Serratì, PhD, Francesca Margheri, PhD, Anastasia Chillà, PhD, Gabriella Fibbi, PhD, Mario Del Rosso, MD: University of Florence and Center for the Study at Molecular and Clinical Level of Chronic, Degenerative, and Neoplastic Diseases to Develop Novel Therapies (DENOTHE), Florence, Italy; [2]Elena Neumann, PhD, Ulf Müller-Ladner, MD: Justus-Liebig University of Giessen, Giessen, Germany and Kerckhoff-Klinik, Bad Nauheim, Germany; [3]Maurizio Benucci, MD: Nuovo Ospedale di San Giovanni di Dio, Florence, Italy.

Drs. Serratì and Margheri contributed equally to this work.

Address correspondence to Mario Del Rosso, MD, Department of Experimental Pathology and Oncology, University of Florence, Viale G. B. Morgagni 50, 50134 Florence, Italy. E-mail: delrosso@unifi.it.

Submitted for publication May 19, 2010; accepted in revised form April 28, 2011.

inhibitors (1). In tumors, uPAR is overexpressed by malignant cells, and uPA can be produced by cancer cells and by tumor-associated stromal and inflammatory cells (4). In tumor invasion, the cell-associated PA system (5) works together with MMPs (6).

In RA, the hypertrophic synovium behaves like a local tumor, invading the joint cavity and eroding cartilage and bone (7). This process is supported by MMPs and uPA produced by the resident and inflammatory cells of arthritic joints (8,9). Urokinase PA and other proteinases are also produced by resident synovial fibroblasts (SFs) (10–12) and released into the joint cavity (13). SFs also express uPAR on their membrane (7,13). The levels of PAI-1 in RA synovial tissue are higher than those in osteoarthritis (OA) synovium (11), and the amounts of PAI-1 produced by cultured RA SFs are higher than those produced by OA SFs and normal SFs (12,14). Plasminogen/plasmin and uPA are critically required in the early phases of autoimmune type II collagen–induced arthritis (15). In particular, plasminogen also promotes infiltration of inflammatory cells into the synovial joint that in turn induce pathologic inflammatory joint destruction by an unrelated mechanism.

The PA system is therefore considered to be involved in the inflammatory remodeling of connective tissues occurring in arthritic joints. The PA activity of human monocytes, chondrocytes, and synoviocytes is regulated by cytokines produced in diseased joints (1). Alternatively, uPA exhibits arthritogenic activity by inducing release of interleukin-6 (IL-6), IL-1β, and tumor necrosis factor α by joint resident and inflammatory cells; this activity may be blocked by a synthetic uPA inhibitor (16).

The uPA–uPAR interaction drives invasion and chemotaxis in different cell types (4,17,18). We previously showed that normal SFs undergo uPA/uPAR-dependent chemotaxis, chemoinvasion, and proliferation (19), and that RA SFs exhibit the fibrinolytic pattern of invasive tumor cells (7). Taken together, this evidence prompted us to verify whether it is possible, by parallel inhibition of both uPA and uPAR in SFs, to block invasion and proliferation of RA SFs, psoriatic arthritis (PsA) SFs, and healthy human SFs in vitro, as well as RA SF cartilage invasion in vivo.

PATIENTS AND METHODS

Patients. Patients with RA, patients with PsA, and healthy control subjects who were matched with the patients for sex and age were used as a source of synoviocytes. For in vitro studies, synovial tissue was obtained from 3 patients with RA (all meeting the criteria of the American College of Rheumatology) (20) and 3 patients with PsA (21) who underwent arthroscopy before joint replacement surgery, and from 3 control subjects who underwent arthroscopy due to knee trauma. The RA synovial tissue used for in vivo implantation into SCID mice was not obtained during arthroscopy but rather was obtained during joint replacement surgery. The study was approved by the local ethics committees, written informed consent was obtained from each subject enrolled, and procedures were performed according to the 1975 Declaration of Helsinki (as revised in 1983) guidelines for human experimentation.

Synovial cell cultures. Synovial tissue was finely minced and subjected to mild proteolytic treatment (0.05% trypsin, 0.5 m*M* EDTA, for 10 minutes at 37°C under gentle shaking; this approach was used because more prolonged treatments altered cell viability). Trypsin was neutralized with fetal calf serum (FCS) (EuroClone). Both cells and tissue debris were plated with RPMI 1640 (EuroClone) supplemented with 10% FCS, 2 m*M* glutamine (EuroClone), and penicillin/streptomycin (EuroClone) and left to adhere overnight. Cultures were then subjected to a new trypsin–EDTA treatment that detached adherent cells while leaving tissue debris adherent to the plate. The average yields were $\sim 150 \times 10^3$ RA SFs and PsA SFs, and 100×10^3 normal SFs. Cells were plated again until confluence (the doubling times were 36 hours for RA SFs and PsA SFs and 72 hours for normal SFs). The monolayer (operatively considered at passage 1) was removed by a trypsin–EDTA solution and frozen in liquid nitrogen (7). The cells were considered type B fibroblast-like synovial cells if staining with anti-CD69, anti-CD14, anti-CD11b, and anti-CD11c monoclonal antibodies was negative and staining for the enzyme UDPGD was positive, and if they had a spindle-shaped, fibroblast-like morphologic appearance. Such features were shared by >95% of cells at passage 1. In total, 3 RA SF, 3 PsA SF, and 3 normal SF populations were obtained and were used within the seventh passage in culture.

Analysis of uPA, uPAR, and PAI-1. SFs (25×10^3) were seeded with 10% FCS in RPMI 1640. At semiconfluence, cells were washed 3 times with serum-free medium, incubated in 0.2% FCS medium until confluence, detached, and counted. Cells were then lysed, replaced in their original wells, and incubated for 1 hour at 4°C to allow exhaustive extraction of potentially undetached material. Cell extracts were centrifuged and stored at −80°C for uPAR assay. Culture media were collected, centrifuged, and stored at −80°C. Aliquots were analyzed for uPAR, uPA, and PAI-1 by commercially available kits (IMUBIND; American Diagnostica). Each sample was evaluated in triplicate and with 2 different dilutions.

Analysis of uPA activity. The activity of uPA was evaluated by zymography of culture media and cell lysates, as previously described (22). Culture media were dialyzed and lyophilized to reach an optimal volume:protein ratio. In some zymograms, amiloride (1 mmole/liter) was incorporated in the underlay to specifically inhibit uPA (23). In some experiments, cell monolayers were treated for 3 minutes at room temperature with 50 m*N* glycine HCl buffer, pH 3.0, containing 0.1*M* NaCl to detach uPAR-bound uPA (24). Zymography was performed with culture medium, acidic wash, and cell lysates from untreated SFs and from SFs treated for 24 hours with 10 n*M* WX-340, a competitive active-site inhibitor of uPA enzy-

matic activity (a kind gift from Wilex, Munich, Germany). The zymograms (3 for each cell type) were evaluated by densitometric comparison between lysis areas.

Proliferation assay. SFs were seeded in 6 multiwell plates (15×10^3 cells/well) with 10% FCS in RPMI 1640. After 24 hours, cells were washed 3 times with serum-free medium and starved in 0.2% FCS medium for an additional 48 hours. Medium was then removed, and cells were incubated for 48 hours in 10% FCS medium, 0.5% FCS medium, and 0.5% FCS medium with 10 n*M* WX-340. Cells were then counted. Other experiments were performed in the presence of uPAR antisense oligonucleotides (ODNs), as described below. Each experiment was performed in triplicate. Proliferation was also evaluated in cell lysates by Western blotting with antibodies to proliferating cell nuclear antigen (PCNA) (LabVision).

Migration/invasion assay. A 48-well microchemotaxis chamber was used as previously described (17). To evaluate invasion, the 8-μm pore filter separating the 2 wells was coated with Matrigel (Becton Dickinson) (50 μg/filter). Test solutions containing WX-340 and/or ODNs were dissolved in culture medium/0.5% FCS and placed in both the upper and lower wells, while 12.5×10^3 cells were added to each upper well. After 5 hours of culture at 37°C, the filter was removed and fixed with methanol. Cell invasion was evaluated by counting spread cells adhering to the lower filter surface (25). Each experiment was performed in triplicate. The mean values of migrated cells were calculated.

In vitro treatment with the anti-uPA inhibitor WX-340 and with uPAR antisense ODN. Preliminary dose-dependence experiments indicated that WX-340 reached optimal inhibiting activity on normal SF Matrigel invasion at 10 n*M*, and that the activity did not increase at higher concentrations (data not shown). WX-340 at 10 n*M* was therefore used in invasion and proliferation experiments. WX-340 at 10 n*M* did not affect cell viability, as shown by trypan blue exclusion assay. The expression of uPAR was inhibited with an 18-mer phosphorothioate antisense ODN (26,27) (US patent no. 5,872,106, Europe patent no. 0772620; Isis Pharmaceuticals product designation Isis 17916; sequence 5′-CGGCGGGTGACCCATGTC-3′). The control was a completely degenerated 18-mer ODN. ODN uptake and stability were enhanced by combining ODNs with a cationic liposome, namely DOTAP (Boehringer Mannheim), as previously described (26,27). Cell cultures were treated daily for 4 days, as previously reported (26,27). On the fourth day, cells were subjected to proliferation and invasion assays, as described above, in the presence of ODNs. Cell viability results were unaffected, as shown by trypan blue exclusion assay performed at 12-hour intervals following the addition of ODNs plus DOTAP.

Quantification of uPA, uPAR, and PAI-1 gene messenger RNA (mRNA) by reverse transcription–polymerase chain reaction (RT-PCR). Urokinase PA, uPAR, and PAI-1 mRNA levels were determined by an internal-based semiquantitative RT-PCR, using procedures previously described (22,28). The

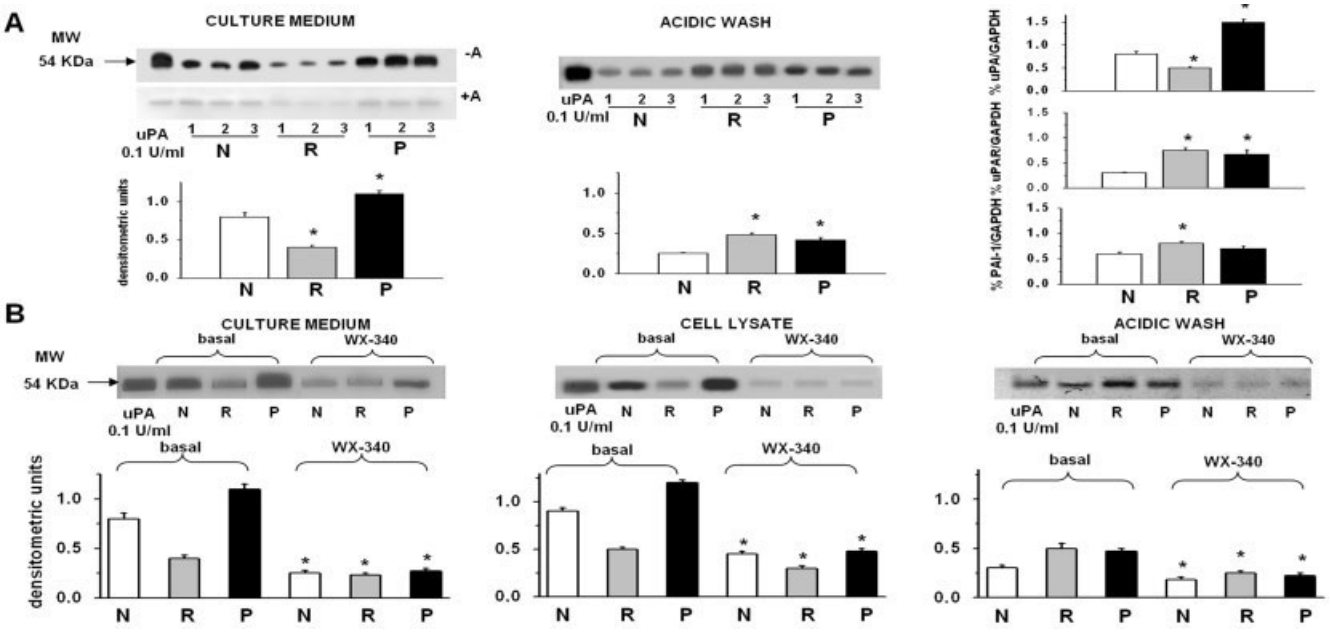

Figure 1. Fibrinolytic activity of normal (N) synovial fibroblasts (SFs), rheumatoid arthritis (RA; R) SFs, and psoriatic arthritis (PsA; P) SFs and its modulation by WX-340. **A,** Left and middle, Results of zymography of plasminogen activators (PAs) performed with culture medium (left) and acidic wash (middle). Three separate experiments for each of the 3 different RA SF, PsA SF, and normal SF cell types were performed (n = 9), without (−A) and with (+A) amiloride. Urokinase PA (uPA) 54 kd was used as the reference standard. Right, Histograms showing quantification of uPA, uPA receptor (uPAR), and PA inhibitor 1 (PAI-1) by reverse transcription–polymerase chain reaction in all the cell types. **B,** Urokinase PA in culture medium (50 μg protein) (left), cell lysates (50 μg protein) (middle), and acidic wash (50 μg protein) (right) of untreated and WX-340–treated SFs. Typical zymograms are shown. Bars show the mean ± SD. $* = P < 0.05$ versus normal SFs (**A**) and versus untreated SFs (**B**).

primer sequences, product size, cycling profile, as well as reaction product analysis and quantification were as previously reported (28). Data are expressed as the percent target molecule: GAPDH ratio.

In vivo experiments and histologic assessment. The SCID mouse model for human RA was used, as previously described (29,30). Four-week-old SCID mice (Charles River) were used. On the day of implantation, normal human cartilage was obtained from the nonarthritic knee joints of patients undergoing routine surgery at the Department of Orthopedics, Markuskrankenhaus, Frankfurt. Implantations were performed under sterile conditions. A synthetic gelatin sponge (30) containing a piece of cartilage was soaked with RA SFs ($\sim 5 \times 10^5$ cells) suspended in sterile saline. Four sponges containing cartilage and RA SFs were inserted under the skin of each anesthetized mouse.

The mice were divided in 6 groups of 4 mice each. Group 1 comprised controls with implants that did not undergo treatment for 60 days. Group 2 comprised mice treated for 60 days with antisense ODN (intraperitoneal injection of 0.5 mg/mouse for 5 days followed by a 2-day interval). Group 3 comprised mice treated according to the same schedule as that for group 2 but with degenerated ODNs. Group 4 comprised mice treated with 0.5 mg/kg WX-340, injected intraperitoneally according to the same schedule described for ODNs. Group 5 comprised mice treated with antisense ODNs plus WX-340. Group 6 comprised mice treated with degenerated ODNs plus WX-340. Two mice were engrafted with inert sponge and cartilage without any RA SFs, to evaluate basal cartilage degradation in the absence of RA SFs. Six mice were also treated with WX-340 (5 mg/kg). The amount of each molecule used in vivo was determined based on previous results obtained with ODNs (25,26) and the in vitro results as well as recommendations of the manufacturer of WX-340. Dissection of the mice took place after 60 days, to evaluate the outcome parameters determined by the treatments.

Using standard hematoxylin and eosin staining, each specimen was evaluated in a blinded manner by 4 independent examiners for the degree of destruction of the implanted cartilage, according to previously described criteria (29,30), as follows: for invasion, 0 = no or minimal invasion, 0.5 = visible invasion ($\sim$2 fibroblast cell depths, 20–30 μm), 1 = invasion ($\sim$5 fibroblast cell depths), 1.5 = deep invasion (5–10 fibroblast cell depths), and 2 = very deep invasion (>10 fibroblast cell depths); for perichondrocytic cartilage degradation, 0 = no degradation (sharp halo), 0.5 = visible degradation (<1 diameter of the chondron), 1 = degradation (1–2 diameters of the chondron), 1.5 = intensive degradation (2–3 diameters of the chondron), and 2 = very intensive degradation (>3 diameters of the chondron).

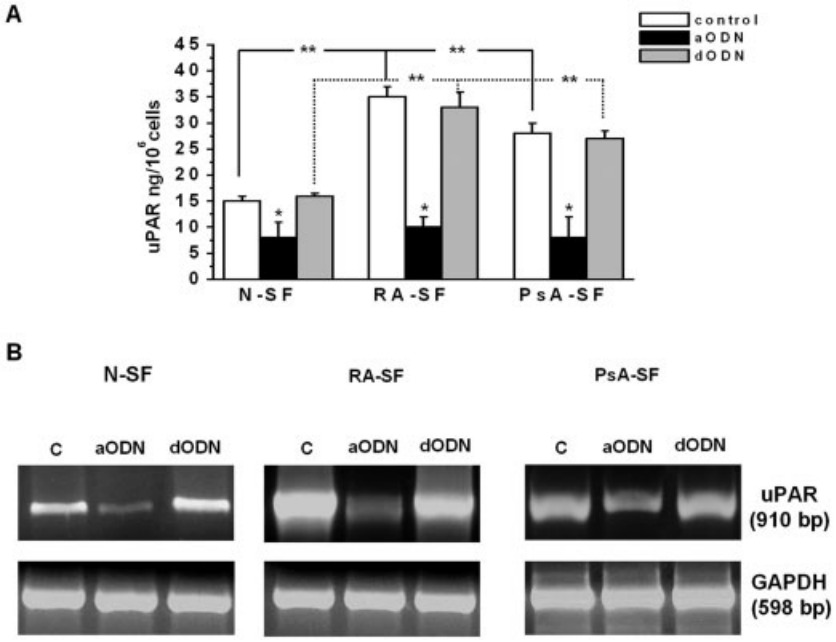

Figure 2. Down-regulation of uPAR in normal SFs, RA SFs, and PsA SFs by uPAR antisense oligonucleotide (aODN). **A,** Extent of uPAR reduction following 4 days of treatment with ODNs, as revealed by enzyme-linked immunosorbent assay. Bars show the mean ± SD of 3 experiments performed in triplicate on each cell line. $* = P < 0.05$ versus control and degenerated ODN (dODN)–treated cells. $** = P < 0.05$, control and degenerated ODN–treated normal SFs versus control and degenerated ODN–treated RA SFs and PsA SFs. **B,** Reduced uPAR mRNA expression following treatment with ODNs, as determined by reverse transcription–polymerase chain reaction. See Figure 1 for other definitions.

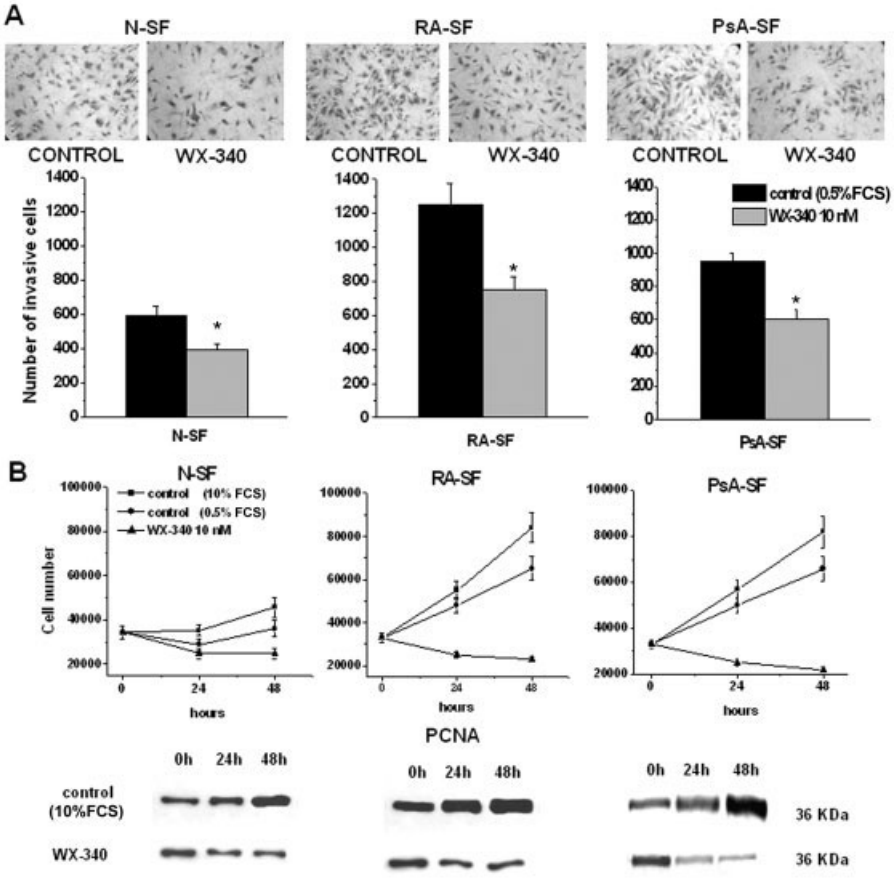

Figure 3. Effect of WX-340 on invasion and proliferation of normal SFs, RA SFs, and PsA SFs. **A,** Top, Photomicrographs showing the migration filters at the end of the assay. Original magnification × 200. **Bottom,** Matrigel invasion of normal SFs, RA SFs, and PsA SFs incubated for 24 hours with 10 n*M* WX-340. Bars show the mean ± SD of 3 experiments performed in triplicate on each cell line. ∗ = $P < 0.05$ versus control. **B,** Top, Proliferation of normal SFs, RA SFs, and PsA SFs in the absence and in the presence of 10 n*M* WX-340. Values are the mean ± SD of 3 experiments performed in triplicate on each cell line. Bottom, Western blotting with antibodies to proliferating cell nuclear antigen (PCNA). FCS = fetal calf serum (see Figure 1 for other definitions).

Statistical analysis. The results are expressed as the mean ± SD of the indicated number of experiments. Comparisons between groups were performed using Student's 2-tailed *t*-tests. *P* values less than 0.05 were considered significant.

RESULTS

Fibrinolytic pattern of normal SFs, PsA SFs, and RA SFs. We previously showed that RA SFs cultured in vitro overexpress uPAR (7). In the current study, we determined expression of the cell-associated fibrinolytic system on normal SFs, PsA SFs, and RA SFs, by enzyme-linked immunosorbent assay (ELISA), zymography, and RT-PCR, in order to characterize the system to be modulated. For zymography, the culture medium of SFs was lyophilized and concentrated 5-fold. As shown in Figure 1A, zymography performed with 30-μl (50 μg protein) aliquots of concentrated culture medium (left panel) and with 60 μl (50 μg protein) of the acidic wash of cell monolayers (middle panel) indicated that RA SFs released lower amounts of active uPA than did healthy nonarthritic controls, and that uPA production was more abundant in PsA SFs, while uPAR-bound uPA (released by the acidic wash) prevailed in both RA SFs and PsA SFs.

The expression of uPA antigens, revealed by ELISA in cell lysates, mirrored the distribution of uPA

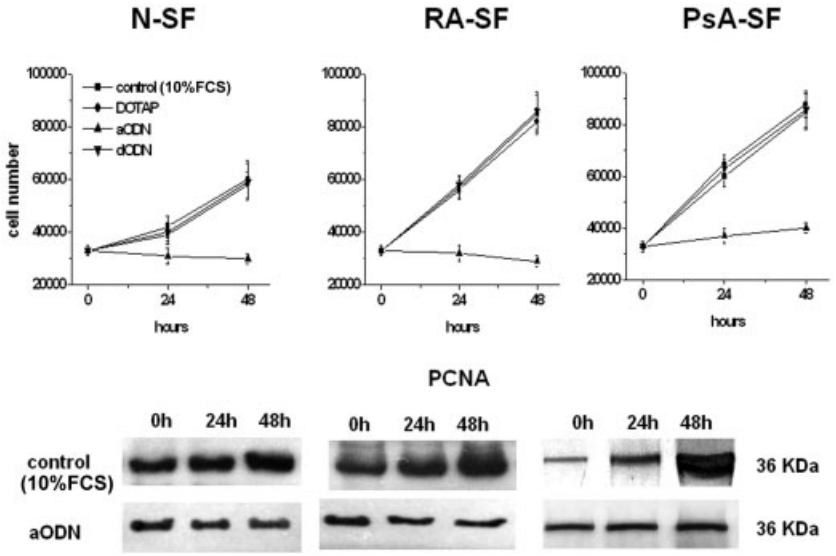

Figure 4. Top, Effect of antisense oligonucleotide (aODN) treatment on proliferation of normal SFs, RA SFs, and PsA SFs, as determined by cell counting. Values are the mean ± SD of 3 experiments performed in triplicate on each cell type. Bottom, Western blotting with antibodies to proliferating cell nuclear antigen (PCNA). FCS = fetal calf serum; dODN = degenerated ODN (see Figure 1 for other definitions).

activity (mean ± SD 11.75 ± 4.25 ng/10^6 cells in normal SFs, 19.6 ± 5.7 ng/10^6 cells in PsA SFs, and 3.1 ± 0.8 ng/10^6 cells in RA SFs; $P < 0.05$ versus normal SFs). The situation was the opposite for uPAR (mean ± SD 34.3 ± 3.8 ng/10^6 cells in RA SFs, 28.7 ± 3.2 ng/10^6 cells in PsA SFs, and 9.25 ± 2.15 ng/10^6 cells in normal SFs; $P < 0.001$ versus normal SFs) and PAI-1 (mean ± SD 7.95 ± 0.8 μg/10^6 cells in RA SFs, 6.88 ± 0.5 μg/10^6 cells in PsA SFs, and 2.3 ± 0.40 μg/10^6 cells in normal SFs; $P < 0.05$ versus normal SFs). In each ELISA (uPA, uPAR, and PAI-1), 3 separate experiments for each of the 3 different RA SF, PsA SF, and normal SF cell types were performed (n = 9). RT-PCR analysis confirmed the data obtained by ELISA (Figure 1A, right panel).

Reduced uPA activity following treatment of normal SFs and RA SFs with WX-340. Zymography was performed with culture media and cell lysates from either untreated SFs or SF cultures maintained for 24 hours in the presence of 10 n*M* WX-340. Although the uPA activity in the culture media of normal SFs, PsA SFs, and RA SFs was only partially affected by the inhibitor, as shown in Figure 1B (left panel), it was reduced in cell lysates (Figure 1B, middle panel). The activity of WX-340 appeared to be higher on uPAR-bound uPA compared with soluble uPA, giving additional value to the inhibiting activity of the compound. To validate this hypothesis, we performed zymographic analysis of aliquots of the acidic wash of normal SFs, PsA SFs, and RA SFs under basal conditions and in the presence of WX-340 (Figure 1B, right panel). The results showed that WX-340–dependent inhibition of uPAR-bound uPA was highly efficient, independently of the cells used. Parallel experiments in which RT-PCR was performed on all of the cell lines indicated that treatment with WX-340 did not affect the expression of either uPA or the other components of the fibrinolysis-associated molecules (uPAR, PAI-1) (results not shown).

Reduced uPAR expression following treatment of normal SFs and RA SFs with uPAR antisense ODN. Gene expression of uPAR was inhibited with an 18-mer phosphorothioate antisense ODN, while a completely degenerated 18-mer phosphorothioate ODN was used as negative control. The uptake and stability of ODNs were enhanced by combining ODNs with a cationic liposome, and SF cultures were treated for 4 days on the basis of preliminary experiments indicating a steady-state reduction of uPAR after 3 days of antisense ODN treatment. The initial treatment with 10 μM cationic lipid–combined ODNs was followed by the addition of 5 μM after 48 hours in order to restore the initial concentration. On the fourth day, cells were detached with EDTA and subjected to measurement of uPAR protein and uPAR mRNA as well as phenotypic

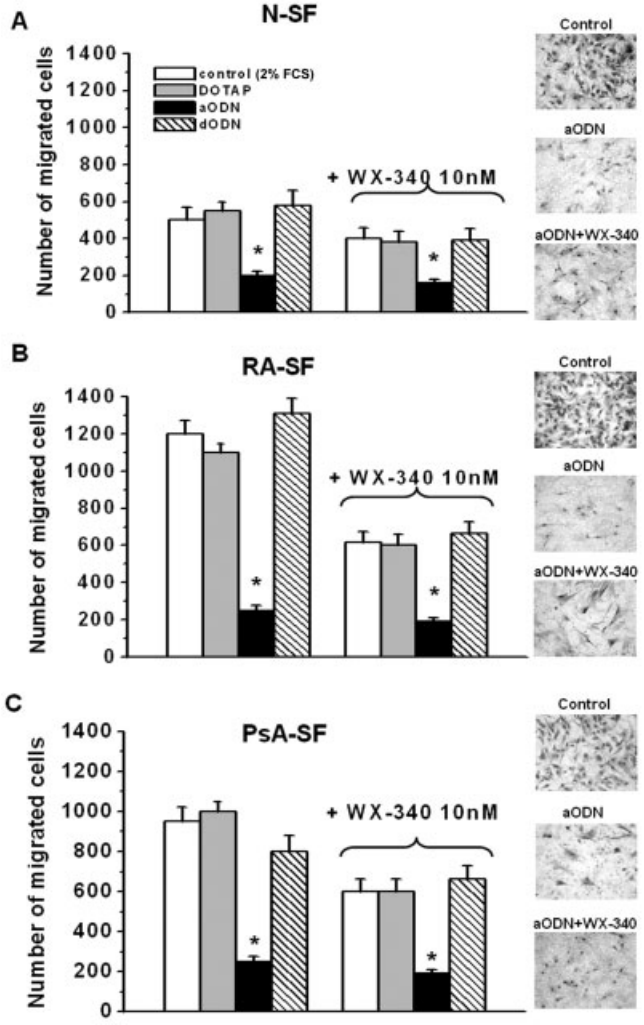

Figure 5. Effect of single treatments (2% fetal calf serum [FCS], DOTAP, antisense oligonucleotide [aODN], and degenerated oligonucleotide [dODN] and combined treatment with WX-340 on Matrigel invasion of normal SFs (**A**), RA SFs (**B**), and PsA SFs (**C**). The photomicrographs show typical patterns of the migration filters at the term of the assay. Original magnification × 200. Bars show the mean ± SD of 3 experiments performed in triplicate on each cell line. * = $P <$ 0.05 versus control. See Figure 1 for other definitions.

analysis (proliferation and invasion). Figure 2A shows the extent of uPAR reduction in normal SFs, RA SFs, and PsA SFs, as revealed by ELISA, while Figure 2B shows the reduced uPAR mRNA expression as determined by RT-PCR.

Inhibition of constitutive invasion and proliferation of normal SFs and RA SFs by WX-340. Cell invasion of Matrigel must be related to the activity of enzymes released from cells or entrapped within the Matrigel itself. The addition of specific enzyme inhibitors may potentially be able to blunt specific enzyme-dependent invasion pathways. On this basis, use of the uPA inhibitor WX-340 is likely to block the contribution of uPA to cell invasion. Figure 3A shows the results obtained by blocking uPA with 10 n*M* WX-340 in the upper and lower compartments of the Boyden chamber. The reduction in Matrigel invasion was greater for RA SFs (mean ± SD 41.7 ± 3.1% inhibition) than for normal SFs (33.7 ± 2.7% inhibition), a consistent difference that was likely attributable to the higher amount of uPAR and uPAR-bound uPA in RA SFs compared with normal SFs. PsA SFs showed 33.4 ± 3.1% inhibition. Constitutive proliferation was also inhibited in normal SFs, RA SFs, and PsA SFs, as evaluated by cell counting and PCNA determination by Western blotting (Figure 3B). It is interesting to note that normal SFs showed lower proliferation than PsA SFs and RA SFs, and that the activity of 10 n*M* WX-340 was relatively more efficient in RA SFs and PsA SFs.

Inhibition of constitutive invasion and proliferation of normal SFs and RA SFs by uPAR antisense ODN. After 3 days of ODN treatment, cells did not show signs of distress. Antisense ODN treatment completely blocked proliferation in normal SFs, RA SFs, and PsA SFs, as shown by cell counting and expression of PCNA (Figure 4). Antisense ODN treatment also inhibited invasion in all types of cells (63.6%, 81.1%, and 74.5% decrease in cell invasion for normal SFs, RA SFs, and PsA SFs, respectively), as shown in Figures 5A–C (left side of each panel).

Effects of combined treatment with WX-340 and uPAR antisense ODN on invasion of normal SFs and PsA SFs. Because the effects of both WX-340 and uPAR antisense ODN on cell proliferation were already maximal, we decided to investigate the cumulative effects of the combined treatment only on cell invasion, which was not completely blocked by either molecule alone, although antisense ODNs were more efficient than WX-340. As shown in Figure 5A (normal SFs), Figure 5B (RA SFs), and Figure 5C (PsA SFs), the cumulative effect of combined treatment was evident in all cell types but was particularly important in RA SFs (87% inhibition compared with 59% and 66% inhibition for normal SFs and PsA SFs, respectively).

In vivo experiments in the SCID mouse model. Figure 6 shows the results of human cartilage invasion by RA SFs in the SCID mouse model of human RA, 60 days after implantation. A reduction of cartilage invasion was observed only with uPAR antisense ODN treatment (alone or combined with WX-340), while all other treatments (alone or combined) were ineffectual

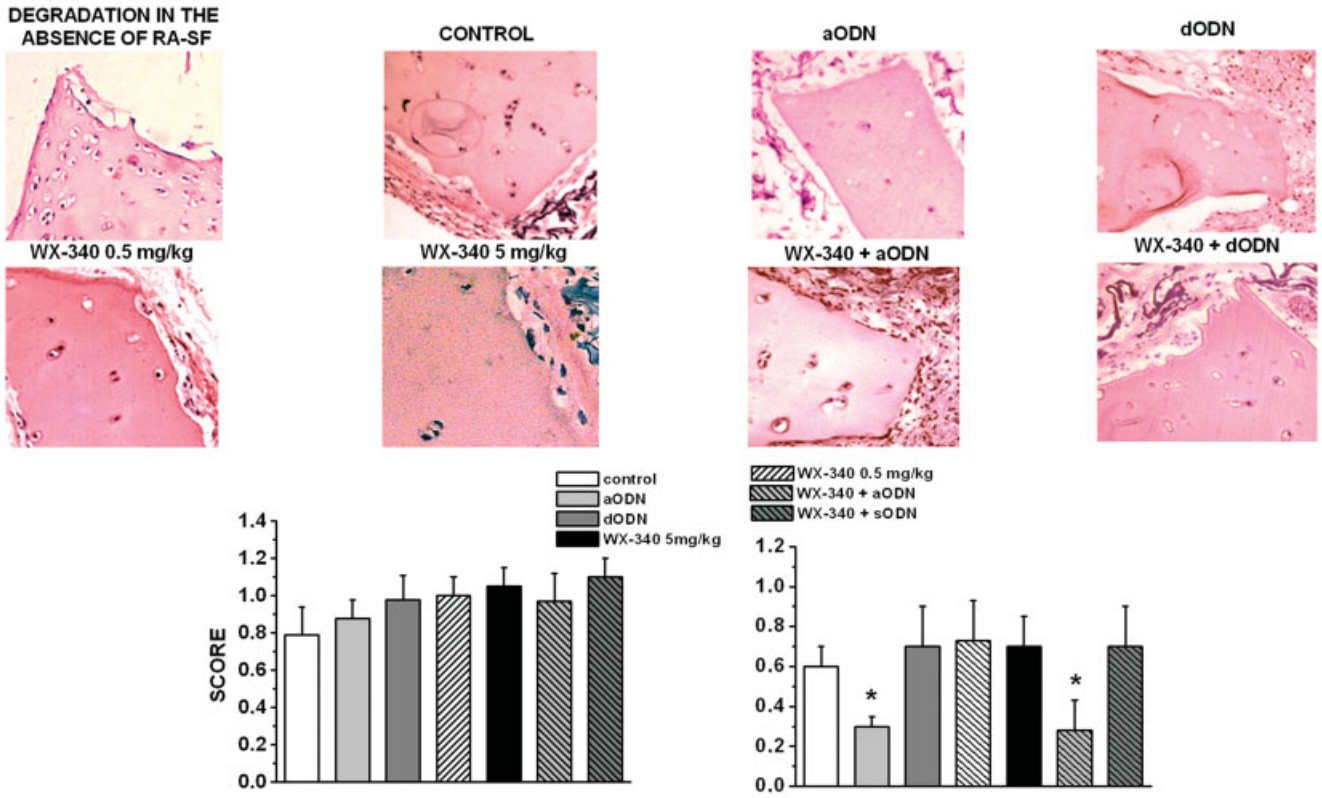

Figure 6. Human cartilage invasion by RA SFs in the SCID mouse model of human RA, 60 days after implantation. Top, Hematoxylin and eosin–stained specimens showing the degree of destruction of implanted cartilage under various treatment conditions. The photomicrographs are representative of 4 replicates in 4 different animals (16 sections for each condition). Original magnification × 200. Bottom, Scores for perichondrocytic degradation (left) and cartilage invasion (right). In the histogram on the right, the score for basal cartilage erosion (occurring in the absence of RA SFs [mean 0.47] soaked in the perichondral sponge) was subtracted from the reported values. Bars show the mean ± SD of 16 sections. $* = P < 0.05$ versus control. aODN = antisense oligonucleotide; dODN = degenerated ODN (see Figure 1 for other definitions).

with respect to control untreated mice. It is noteworthy that even pieces of human cartilage implanted without RA SFs showed appreciable erosion, the extent of which was evaluated according to the parameters described in Materials and Methods (see Figure 6). For all reported values, the score of 0.47 (the average score of cartilage degradation in the absence of RA SFs within the sponge) has been subtracted. Perichondrocytic cartilage degradation was unaffected under all conditions. It is noteworthy that WX-340 treatment was ineffective even when the concentration of the daily intraperitoneal injection was increased 10-fold (from 0.5 mg/kg/mouse to 5.0 mg/kg/mouse).

DISCUSSION

In this study, we examined the effects of 2 inhibitory strategies against the fibrinolytic system on the in vitro and in vivo invasive properties of normal SFs, PsA SFs, and RA SFs. We showed that invasion and growth of all cell types in vitro depend on the expression of uPA and its receptor uPAR. Overexpression of uPAR on RA SFs and PsA SFs determines preferential partitioning at the cell membrane of secreted uPA, which accounts for their more intense invasion and growth. The single and/or combined use of uPAR antisense and of a small molecule that inhibits uPA activity reduced these invasion and proliferation properties in vitro, while only the antisense approach reduced cartilage invasion of RA SFs in a SCID mouse model.

Previous studies have shown that SFs, as well as other resident joint cells, secrete PAs and PAIs and express uPAR on their membrane (1,7,11,13,19). Moreover, RA SFs have been shown to overexpress uPAR, a feature that resembles the proinvasive pattern of malig-

nant cells (7). Therefore, the fibrinolytic system has been thought to be involved in the pathogenesis of tissue remodeling that characterizes degradative joint pathologies, such as RA and PsA. However, no direct experimental evidence has been provided so far about its functions in SFs. Previous observations (11,13) indicated overexpression not only of uPAR and PAI-1 but also of uPA in the synovial tissue of patients with RA. However, because data on the up-regulation of all components of the fibrinolytic system were obtained from tissue specimens, not isolated synovial cells cultured as monolayer in vitro, the present experiments showed the unique alterations of RA SFs as RA-driving cells.

Under in vivo conditions, the evidence of larger amounts of uPA in RA SFs may be the product of the complex cytokine crosstalk occurring within the inflammatory environment of the arthritic joint. This suggests that RA SFs may bind uPA that is produced by other cells (such as monocytes and chondrocytes) or is overproduced by other synovial cells under the effect of inflammatory cytokines (30–33). Our experiments revealed that the higher expression of uPAR on RA SFs allows a higher surface association of uPA, independent of uPA released by cells into the culture medium. The reduction of uPA in the culture medium of RA synoviocytes must therefore be related to reduced uPA gene expression as well as to a differential uPA partitioning and uPA/uPAR complex formation on SF membrane.

Although PsA is a seronegative inflammatory joint disease, its aggressive bone resorption is similar to that occurring in RA. Here we showed overexpression of uPAR, uPA, and PAI-1 in PsA SFs and the possibility of controlling their proliferation and invasion by uPA/uPAR inhibition. These results indicated that although uPA/uPAR-dependent proliferation and invasion of SFs are prominent features of RA SFs, the extent to which the cell-associated fibrinolytic system contributes to joint damage is comparable in RA and PsA.

On this basis, in an attempt to inhibit the proliferative and invasive activity of SFs, we tried to primarily block the SF fibrinolytic system. We compared the inhibition of proliferation and invasion by an inhibitor of uPA enzymatic activity (WX-340) and by an antisense ODN inhibitor of uPAR expression, as well as their cumulative effects. First, the addition of WX-340 to the culture medium of normal SFs, PsA SFs, and RA SFs resulted in a strong reduction of the activity of cell-associated uPA, while a weak effect was observed on uPA present in the culture medium. The use of uPAR antisense ODN produced a reduction of uPAR expression in all SF types at both the protein and RNA levels. WX-340 alone inhibited Matrigel invasion by SFs. The same compound was extremely efficient in blocking SF growth, a property that was particularly evident in RA SFs and PsA SFs. Of note, the use of uPAR antisense ODN was even more effective in inhibiting SF invasion.

Because growth inhibition by WX-340 and uPAR antisense ODN on SFs was already maximal, we evaluated the cumulative effect of combined treatment with WX-340 and uPAR antisense ODN only on cell invasion. The combined treatment was particularly efficient in RA SFs and PsA SFs. The decrease in the cell amount observed between time 0 and time 24 (as shown in Figures 3 and 4) was related to a temporary weakening of cell adhesion ascribable to inhibition of the uPA/uPAR-dependent grip, as reported elsewhere (27). These data support the idea that therapeutic attempts to inhibit the constitutive proliferation and invasion of RA SFs must consider the inhibition of both uPA and of its receptor, which both independently and coordinately contribute to the proliferative and invasive properties of the rheumatoid synovium. However, human cartilage invasion by RA SFs in the SCID mouse model of human RA showed that antisense ODN–dependent inhibition of uPAR expression alone was sufficient to induce a 55% reduction of cartilage invasion, while WX-340 did not show any efficacy, either alone or in combination with antisense ODN. It is noteworthy that differences in perichondrocyte cartilage degradation, which often is present at areas where the invasive synovial pannus contains local concentrations of mast cells or exceptionally dense distribution of inflammatory cells (34), were not observed under our experimental conditions.

In summary, we have shown that normal SF and RA SF invasion and growth are decreased by inhibiting the function of the cell-associated fibrinolytic system. A competitive active-site inhibitor of uPA activity (WX-340) and uPAR antisense ODN could inhibit Matrigel invasion and proliferation of RA SFs in vitro, predominantly when both antagonizing molecules were simultaneously added to the experimental culture medium. Of interest, when the 2 compounds were used to inhibit human cartilage invasion and degradation by RA SFs in the SCID mouse model of RA, only the antisense ODN approach was effective, even when WX-340 was used at 10-fold concentrations (Figure 6). These results do not rule out the utility of uPA inhibitors within RA joints. When WX-340 is administered systemically, its biodistributive properties and/or stability may be inadequate to allow sufficient accumulation in the target model used. However, taking into account the high in vitro activity of WX-340 on RA SFs, we hypothesize that a

local intrajoint injection of the inhibitor may be used in a therapeutic attempt to control RA cartilage erosion.

These results also underline the value of the SCID mouse model in testing strategies for antirheumatic therapy, because treated mice tolerated the 60-day intraperitoneal treatment without showing signs of distress.

AUTHOR CONTRIBUTIONS

All authors were involved in drafting the article or revising it critically for important intellectual content, and all authors approved the final version to be published. Dr. Del Rosso had full access to all of the data in the study and takes responsibility for the integrity of the data and the accuracy of the data analysis.

Study conception and design. Serratì, Margheri, Chillà, Neumann, Müller-Ladner, Benucci, Fibbi, Del Rosso.

Acquisition of data. Serratì, Margheri, Chillà, Neumann, Müller-Ladner, Benucci, Fibbi, Del Rosso.

Analysis and interpretation of data. Serratì, Margheri, Chillà, Neumann, Müller-Ladner, Benucci, Fibbi, Del Rosso.

REFERENCES

1. Del Rosso M, Fibbi G, Matucci-Cerinic M. The urokinase-type plasminogen activator system and inflammatory joint diseases. Clin Exp Rheumatol 1999;17:485–98.
2. Ludwig T. Local proteolytic activity in tumor cell invasion and metastasis. Bioessays 2005;27:1181–91.
3. Van Hinsbergh VW, Engelse MA, Quax PH. Pericellular proteases in angiogenesis and vasculogenesis. Arterioscler Thromb Vasc Biol 2006;26:716–28.
4. Del Rosso M, Fibbi G, Pucci M, D'Alessio S, Del Rosso A, Magnelli L, et al. Multiple pathways of cell invasion are regulated by multiple families of serine proteases. Clin Exp Metastasis 2002;19:193–207.
5. Dano K, Behrend N, Hoyer-Hansen G, Johnsen N, Lund LR, Ploug M, et al. Plasminogen activation and cancer. Thromb Haemost 2005;93:676–81.
6. Whitelock JM, O'Grady RL, Gibbins JR. Interstitial collagenase (matrix metalloproteinase 1) associated with the plasma membrane of both neoplastic and nonneoplastic cells. Invasion Metastasis 1991;11:139–48.
7. Guiducci S, Del Rosso A, Cinelli M, Margheri F, D'Alessio S, Fibbi G, et al. Rheumatoid synovial fibroblasts constitutively express the fibrinolytic pattern of invasive tumor-like cells. Clin Exp Rheumatol 2005;23:364–72.
8. Okamoto H, Cujec TP, Yamanaka H, Kamatani N. Molecular aspects of rheumatoid arthritis: role of transcription factors. FEBS J 2008;257:4463–70.
9. Busso N, Hamilton JA. Extravascular coagulation and the plasminogen activator/plasmin system in rheumatoid arthritis [review]. Arthritis Rheum 2002;46:2268–79.
10. Judex MO, Mueller BM. Plasminogen activation/plasmin in rheumatoid arthritis: matrix degradation and more. Am J Pathol 2005;166:645–7.
11. Ronday HK, Smits HH, Van Muijen GN, Pruszczynski MS, Dohlain RJ, Van Langelaan EJ, et al. Difference in expression of plasminogen activation system in synovial tissue of patients with rheumatoid arthritis and osteoarthritis. Br J Rheumatol 1996;35:416–23.
12. Matucci Cerinic M, Generini S, Partsch G, Pignone A, Dini G, Konttinen YT, et al. Synoviocytes from osteoarthritis and rheumatoid arthritis produce plasminogen activators and plasminogen activator inhibitor-1 and display u-PA receptor on their surface. Life Sci 1998;63:441–53.
13. Busso N, Peclat V, So A, Sappino AP. Plasminogen activation in synovial tissues: differences between normal, osteoarthritis, and rheumatoid arthritis joints. Ann Rheum Dis 1997;56:550–7.
14. Watanabe N, Ando K, Yoshida S, Inuzuka S, Kobayashi M, Matsui N, et al. Gene expression prolife analysis of RA-SF cultures revealing the overexpression of genes responsible for tumor-like growth of rheumatoid synovium. Biochem Biophys Res Commun 2002;294:1121–9.
15. Li J, Ny A, Leonardsson G, Nandakumar KS, Holmdahl R, Ny T. The plasminogen activator/plasmin system is essential for development of the joint inflammatory phase of collagen type II-induced arthritis. Am J Pathol 2005;166:783–92.
16. Jin T, Tarkowski A, Carmeliet P, Bokarewa M. Urokinase, a constitutive component of the inflamed synovial fluid, induces arthritis. Arthritis Res Ther 2003;5:R9–17.
17. Fibbi G, Ziche M, Morbidelli L, Magnelli L, Del Rosso M. Interaction of urokinase with specific receptors stimulates mobilization of bovine adrenal capillary endothelial cells. Exp Cell Res 1988;179:385–95.
18. Del Rosso M, Fibbi G, Schmitt M. Non-enzymatic activities of proteases: from scepticism to reality. Biol Chem 2002;383:1–4.
19. Fibbi G, Pucci M, Serni U, Matucci Cerinic M, Del Rosso M. Antisense targeting of the urokinase receptor blocks urokinase-dependent proliferation, chemoinvasion, and chemotaxis of human synovial cells and chondrocytes in vitro. Proc Assoc Am Phys 1998;110:340–50.
20. Aletaha D, Neogi T, Silman AJ, Funovits J, Felson AT, Bingham CO, et al. 2010 rheumatoid arthritis classification criteria. Arthritis Rheum 2010;2:2569–81.
21. Taylor W, Gladman D, Helliwell P, Marchesoni A, Mease P, Mielants H. Classification criteria for psoriatic arthritis: development of new criteria from a large international study. Arthritis Rheum 2006;54:2665–73.
22. Serrati S, Margheri F, Fibbi G, Di Cara G, Minafra L, Pucci-Minafra I, et al. Endothelial cells and normal breast epithelial cells enhance invasion of breast carcinoma cells by CXCR-4-dependent up-regulation of urokinase-type plasminogen activator receptor (uPAR, CD87) expression. J Pathol 2008;214:545–54.
23. Jankun J, Skrzypczak-Jankun E. Molecular basis of specific inhibition of urokinase plasminogen activator by amiloride. Cancer Biochem Biophys 1999;17:109–23.
24. Stoppelli MP, Tacchetti C, Cubellis MV, Corti A, Hearing VJ, Cassani G, et al. Autocrine saturation of pro-urokinase receptors on human A431 cells. Cell 1986;45:675–84.
25. D'Alessio S, Fibbi G, Cinelli M, Guiducci S, Del Rosso A, Margheri F, et al. Matrix metalloproteinase 12–dependent cleavage of urokinase receptor in systemic sclerosis microvascular endothelial cells results in impaired angiogenesis. Arthritis Rheum 2004;50:3275–85.
26. Quattrone A, Fibbi G, Anichini E, Pucci M, Zamperini A, Capaccioli S, et al. Reversion of the invasive phenotype of transformed human fibroblasts by anti-messenger oligonucleotide inhibition of urokinase receptor gene expression. Cancer Res 1995;55:90–5.
27. Margheri F, D'Alessio S, Serrati S, Pucci M, Annunziato F, Liotta F, et al. Effects of block urokinase receptor signaling by antisense oligonucleotides in a mouse model of experimental prostate cancer bone metastases. Gene Ther 2005;12:702–14.
28. Serrati S, Margheri F, Pucci M, Cantelmo AR, Cammarota R, Dotor J, et al. TGFβ1 antagonistic peptides inhibit TGFβ1-dependent angiogenesis. Biochem Pharmacol 2009;77:813–25.
29. Judex M, Neumann E, Fleck M, Pap T, Mountz JD, Gay RE, et al.

"Inverse wrap": an improved implantation technique for virus-transduced synovial fibroblasts in the SCID mouse model for rheumatoid arthritis. Mod Rheumatol 2001;11:145–50.
30. Lefevre S, Knedla A, Tennie C, Kampmann A, Wunrau C, Dinser R, et al. Synovial fibroblasts spread rheumatoid arthritis to unaffected joints. Nat Med 2009;15:1414–20.
31. Hamilton JA, Slyvka J. Stimulation of human synovial fibroblast plasminogen activator production by mononuclear cell supernatants. J Immunol 1981;126:851–5.
32. Hart PH, Vitti GF, Burgess DR, Whitty GA, Royston K, Hamilton JA. Activation of human monocytes by granulocyte-macrophage colony-stimulating factor: increased urokinase-type plasminogen activator activity. Blood 1991;77:841–8.
33. Vitti G, Hamilton JA. Modulation of urokinase-type plasminogen activator messenger RNA levels in human synovial fibroblasts by interleukin-1, retinoic acid, and a glucocorticoid. Arthritis Rheum 1988;31:1046–51.
34. Wolley DE, Tetlow LC. Observations on the microenvironmental nature of cartilage degradation in rheumatoid arthritis. Ann Rheum Dis 1997;56:151–61.